
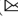







Optimized Performance Pulse Oximeter Based on the MAX30102 Commercial Sensor

Ricardo Cebada-Fuentes¹  , José Valladares-Pérez¹ ,
José Antonio García-García² , and Celia Sánchez-Pérez¹ 

¹ Instituto de Ciencias Aplicadas y Tecnología, Universidad Nacional Autónoma de México, Ciudad de México 04510, Mexico

ricardo.cebada@icat.unam.mx

² Hospital General de México “Dr. Eduardo Liceaga”, Dirección de Educación y Capacitación en Salud, Ciudad de México 06720, Mexico

Abstract. Pulse oximeters are devices that use the photoplethysmography technique to estimate oxygen saturation in blood and heart rate. The MAX30102 is a sensor for reflective photoplethysmography with signal-conditioning and digitalization stages embedded in a single chip that facilitate its implementation in wearable devices. However, there are limitations and external factors that affect its performance in a significant way. This paper suggests a pulse oximeter based on the MAX30102 whose performance has been optimized through the design of algorithms adapted to the signals of this particular sensor. The performance of two heart rate measurement algorithms is compared, one based on a pulse counter and the other on the Fast Fourier Transform (FFT). The proposal covers from the algorithms design to the manufacture of a functional prototype tested with volunteers. Results indicate an accuracy of $\pm 1.39\%$ for the measurement of oxygen saturation and ± 2.04 bpm for heart rate. The Bland-Altman analysis of the pilot test results indicate that prototype measurements are comparable to those of a high-end oximeter taken as reference.

Keywords: MAX30102 · Photoplethysmography · Pulse oximetry · FFT · Bland-Altman

1 Introduction

Photoplethysmography is a non-invasive technique that allows the estimation of the amount of oxygenated hemoglobin (HbO_2) in blood respect to total hemoglobin. It consists in applying light at different wavelengths, typically red ($\lambda = 660$ nm) and infrared ($\lambda = 880$ nm), in an area of the body irrigated with arterial blood to analyze the attenuated light by absorption due to the different tissues through which it passes [2]. The detection of this dimmed light produces a variable amplitude signal called photoplethysmogram signal or PPG, which

has a continuous intensity (DC) and a pulsatile intensity (AC) components [1]. Pulse oximeters use this technique to determine oxygen saturation (SpO_2) and heart rate (HR) quickly and continuously.

During Covid-19 pandemic, the use of pulse oximeters became an obligatory practice among physicians for the monitoring of patients, both in hospitals and remotely [3]. The Pan-American Health Organization (PAHO) has established the technical and functional specifications that clinical pulse oximeters must follow. As technical requirements, it is pointed out that SpO_2 and HR measurements must be carried out with a minimum accuracy of $\pm 3\%$ and ± 3 bpm, respectively, as well as with a one-unit resolution [9]. Among the most important features required are the display of the photoplethysmography waveform, visual and audible alarms for out-of-range measurements, charging indicator, battery status, signal quality indicator and internal data storage [9].

The MAX30102 is a reflection-type photoplethysmography sensor widely used in the development of wearable devices. One of its advantages is that it integrates within the same chip, a conditioning and digitalization stage for the PPG signal that reduces the number of electronic components necessary to implement this sensor in a practical application. Similarly, its intrinsic operating parameters such as sampling rate (SR), LED current (I_{LED}), pulse width and analog to digital converter resolution (ADC) are fully programmable to the user by modifying memory registers via the I^2C protocol [10]. Obtaining a good quality PPG signal with this sensor depends to a great extent on finding an optimal combination of these parameters.

There are several works in which the development of pulse oximeters based on the MAX30102 is suggested, however, very few of them address the search for an optimal configuration of its intrinsic parameters and the design of SpO_2 and HR calculation algorithms appropriate to the particularities of this sensor in which its limitations are taken into account [5,6]. Similarly, few papers address the development of a complete pulse oximeter from the algorithms design to the manufacture of a fully functional prototype that meets the PAHO requirements and that has been subjected to tests with users [13].

In this paper, an optimized performance finger pulse oximeter based on the MAX30102 is presented. This performance optimization is achieved by two ways. The first one, is to obtain the optimal values for the intrinsic parameters LED current (I_{LED}) and sampling rate (SR), with which a high quality PPG signal is obtained. The second way is the development of SpO_2 and HR calculation algorithms adequate for the MAX30102 signals considering both the sensor and microcontroller limitations. Under this approach, the performance of two HR calculation algorithms is compared, one based on the analysis of the PPG signal intensity, and the other, based on a frequency analysis. Finally, a pilot test of the prototype functioning is carried out in a group of 15 healthy people comparing it with a high-end commercial oximeter.

2 Design and Implementation

2.1 General Description of the Developed Pulse Oximeter

The design of the proposed pulse oximeter was performed taking various commercial oximeters as models and considering key elements such as ergonomics and finger restrain mechanisms. The outer case of the prototype was manufactured using 3D printing with polylactic acid polymers (PLA) and thermoplastic polyurethane (TPU) and is held together by a screw-spring mechanism that exerts an adjustable pressure on the finger. Finding the right magnitude for this pressure is one of the key factors that determine the quality of the PPG signal, since excessive pressure will completely deform it.

Some of the main operating features of this prototype are the display of the photoplethysmography waveform, bluetooth connectivity for data storage, visual and audible alarms for SpO_2 and/or HR out-of-range measurements, charge monitor and battery status, signal intensity indicator and battery charge via a USB-C connection. These features fully comply with the functionality requirements established by PAHO [9].

For the development of the pulse oximeter an ESP32 Expressif Systems microcontroller was used as the central processing unit. Figure 1 shows the functional prototype in operation.

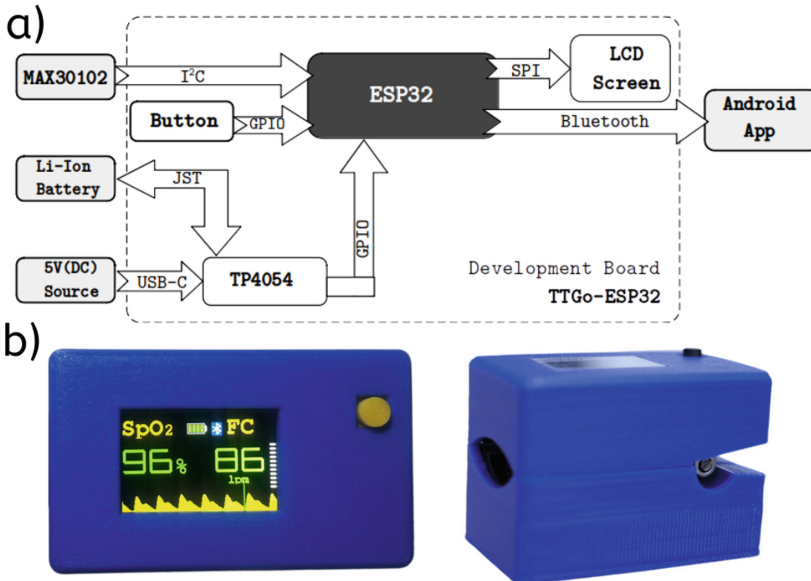


Fig. 1. a) Block diagram of the interconnection of the prototype components. b) Functional prototype operating.

2.2 Acquisition and Conditioning of the PPG Signal

The acquisition of PPG signals is done digitally through the I^2C protocol. Since the sensor has an embedded conditioning stage, there is no need for additional electronic components as post processing is done digitally. Because the proposed algorithms for calculating HR are design to work with the pulsatile components, an IIR type digital low-pass filter was implemented with a cut-off frequency $f_c = 0.05$ Hz.

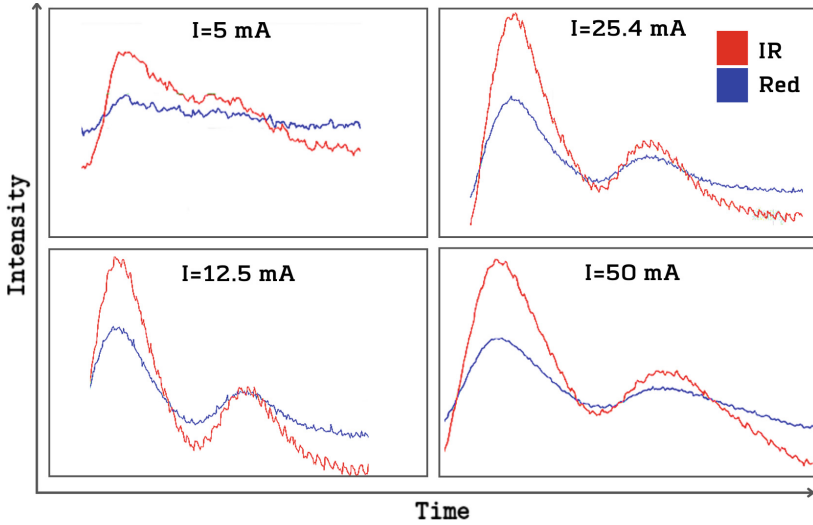


Fig. 2. Quality of PPG signal for different I_{LED} values.

One of the parameters that determine the PPG signal quality is the brightness intensity of the light emitting sources, which is directly linked to the current intensity supplied to them. In the MAX30102, this current can be varied between 0 and 50 mA at intervals of 0.2 mA and it was determined that the best signal quality is obtained for values greater than 40 mA. Lower current values can cause deformities in the PPG signal or produce higher noise levels (Fig. 2) that would affect the performance of the measurement algorithms.

2.3 SpO_2 Calculation

The calculation of oxygen saturation is based on the fact that oxygenated (HbO_2) and deoxygenated (Hb) hemoglobin have different absorption properties for visible and infrared wavelengths. This difference allows to estimate the proportion of HbO_2 to total hemoglobin in arterial blood from the value of the ratio of ratios (R) of the AC and DC components [4] (Eq. 1).

$$R = \frac{(AC_{rms}/DC)_R}{(AC_{rms}/DC)_{IR}} \quad (1)$$

The relationship between R and SpO_2 is determined experimentally through ABG (*Arterial Blood Gas*) tests in volunteers with which a linear approximation of Lambert-Beer law is obtained (Eq. 2). The values of the coefficients α and β depend on the type of sensor and are usually provided by the manufacturer in the sensor's datasheet. In the case of the MAX30102 the values of these coefficients are $\alpha = -17$ y $\beta = 104$ [7].

$$\%SpO_2 = \alpha R + \beta \quad (2)$$

2.4 Heart Rate Calculation

The heart rate (HR) indicates the number of heart beats within a minute and is calculated from the frequency of the PPG signal. There are several methods to determine this frequency but in general they can be classified into two categories: methods that analyze the intensity of the signal and methods that perform decomposition into frequencies. Both methods were studied in this paper with a particular approach in the MAX30102 to determine its advantages and limitations in a practical implementation.

The methods of intensity analysis consist mainly of detection and peak counting algorithms that require few computational resources but are susceptible to failures in the presence of noise. It has been noted that two of the factors affecting the performance of the MAX30102 are movement in the measurement area and low blood perfusion [11]. The movement deforms the PPG signal by inducing fake peaks and sudden amplitude changes, while low perfusion causes significant attenuation on the pulse's amplitude and an increase in the base noise level. That is why the suggested algorithm seeks to detect these alterations on the PPG signal and discriminate them in the final calculation of the HR so as not to affect the measurement.

The proposed algorithm comprises a peak detection stage inspired by an algorithm proposed by Arguello, to which a number of additional conditions have been added to improve the detection for the specific case of the MAX30102 signals [14]. This algorithm works under the assumption that a PPG signal is a strictly increasing function. That is, if the function is denoted by f , then all the points that make it up fulfill the following condition in time (t):

$$f(t_{i+1}) > f(t_i) \quad \text{if} \quad t_{i+1} > t_i \quad (3)$$

A peak is detected when a sign change occurs on the slope of the signal. To differentiate a systolic peak from a diastolic one the algorithm counts the number of times that the condition of Eq. 3 (*num_upsteps*) is met and evaluates whether this number of occurrences reaches a threshold value, in which case it is concluded that a peak has been detected. Because PPG signals have amplitude variations, this threshold is recalculated dynamically according to the total number of samples that make up the rising flank of a systolic peak and which depends on the sampling rate (SR) of the sensor.

One of the additional conditions proposed compares the amplitude of a signal sample ($samp(i)$) with a threshold value (PPG_{MV}) that is equal to 1.5 times the

mean value of the PPG signal calculated for a 50-second window that is updated in real time. This allows to improve the detection of pulses in the presence of slight movements and low intensity noise. Similarly, it was added a condition for resetting the threshold value when there is a substantial increase in the amplitude of the signal due to sudden movement. The flow chart of the suggested algorithm is shown in Fig. 3.

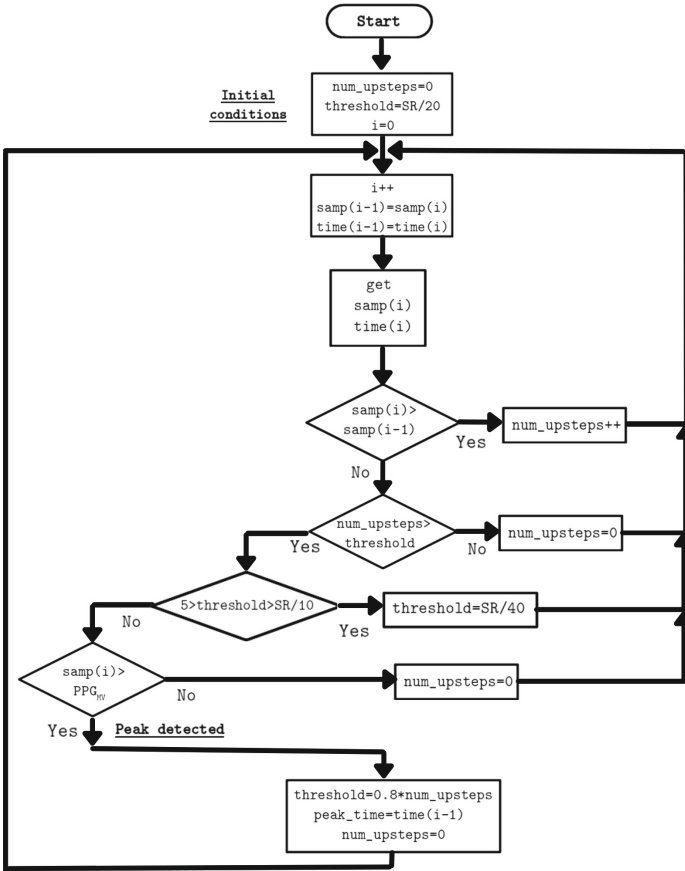


Fig. 3. Flowchart of the proposed algorithm for the detection of peaks in the PPG signal for later use in the calculation of HR.

Unlike the methods used in the intensity based analysis, the frequency methods perform a spectral decomposition of the signal in its fundamental components by using algorithms such as the Discrete Fourier Transform (DFT). In practice, DFT is solved by optimized algorithms such as the Fast Fourier Transform (FFT) which greatly reduces the number of operations required [15]. Some research where the FFT has been used to calculate HR point out that the results

are very similar to those obtained with pulse counting algorithms [16]. For this research, the applied FFT algorithm was a 512-point radix-2 Cooley-Tukey algorithm.

An important advantage of this method is that it has a higher noise immunity compared to pulse counters, however, to calculate HR with the desired resolution of 1 bpm it is necessary for the FFT to calculate the PPG signal frequency with a minimum resolution of 0.016 Hz. This means that the number of data (N) required for a given sampling rate (SR) and frequency bin (N_{bin}), has to be very large, as indicated in Eq. 4 [17]. In a practical implementation this represents a disadvantage due to SRAM memory limitations of the used microcontroller.

$$f_{FFT} = N_{bin} \frac{SR}{N} \quad (4)$$

In the case of MAX30102, in order to maximize the FFT resolution, the maximum possible sample rate of the sensor ($SR = 50$ mps) should be used. Preliminary tests with the ESP32 showed that the largest number of floating point variables that can be stored for the implemented FFT is 512, which implies that the maximum resolution in the frequency calculation is 0.097 Hz, equivalent to 5.8 bpm in heart rate units.

2.5 Comparison of HR Calculation Algorithms

To evaluate the operation of the proposed algorithms, a series of computer tests were carried out with simulated PPG signals for different HR and SNR (*Signal to Noise Ratio*) values and it was concluded that the FFT had a better performance in presence of noise and movement than the intensity algorithm as expected (Fig. 4), however, because of the limited SRAM memory in the microcontroller, the 5.8 bpm resolution in the calculation of the HR does not meet the PAHO requirement of one-unit resolution. For this reason, it was decided to use the intensity based algorithm in the in the final prototype.

3 Results

A series of validation tests were performed to determine the accuracy of the prototype. SpO_2 and HR measurements were compared with those of a high-end commercial oximeter model Masimo[®] MightySat. Table 1 shows a summary of the absolute ($\overline{\varepsilon_a}$) and relative ($\overline{\varepsilon_r\%}$) average errors obtained after testing the final prototype on a healthy volunteer. The results indicate accuracies of 1.39% and 2.04 bpm for SpO_2 and HR, respectively, which clearly meets the PAHO requirements.

To evaluate the performance of the prototype in a real environment, it was considered necessary to carry out a pilot study in a small sample of healthy people.

To carry out this study, verbal informed consent was obtained from the participants, which is authorized in Mexico for minimal risk and non-invasive research

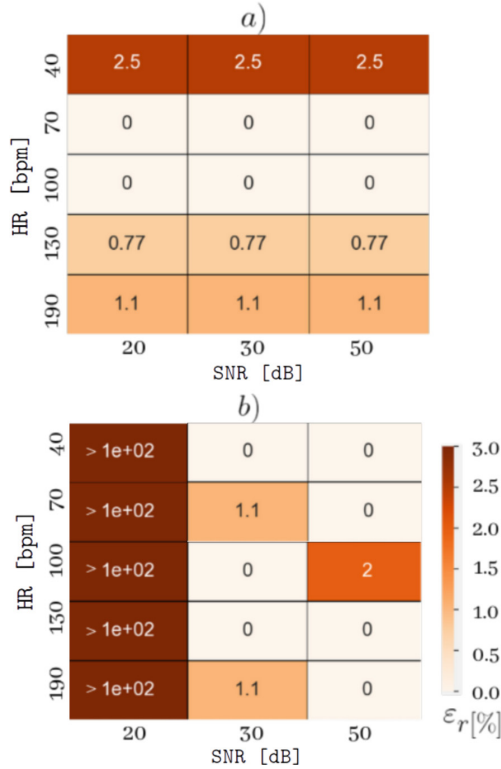


Fig. 4. Heatmap of the relative error $\varepsilon_r\%$ in the calculation of HR performed with simulated PPG signals with different combinations of HR and SNR values using a) 512 point FFT and b) intensity based algorithm.

such as pulse oximetry, as indicated in articles 17 and 23 of Chap. 1 of the Mexican General Health Law [12].

The performance of the prototype was compared with that of the same high-end oximeter used in the validation tests. A total of 15 people participated in the test. 60% were female and the rest were male. The average age was 41 years (± 16) and the third part of the sample said they had suffered from COVID-19 in the last year.

Experimental methodology: 3 measurements were taken for each test subject. Both oximeters were placed simultaneously on the right hand: the prototype on the index finger and the reference on the middle finger. The first measurement was recorded one minute after placing the oximeters, the second, passed 3 min, and the third after 5 min.

Based on the results obtained, a concordance analysis was done using the Bland-Altman method, in which concordance limits are established to study the level of agreement between two instruments or measurement methods. After applying the Student’s T-test to the sample, it was observed that the difference

Table 1. Absolute ($\overline{\varepsilon_a}$) and relative ($\overline{\varepsilon_r\%}$) errors in the measurement of SpO_2 and HR with the working prototype.

Variable	$\overline{\varepsilon_a}$	$\overline{\varepsilon_r\%}$
SpO_2	1.39 %	1.49
HR	2.04 bpm	2.31

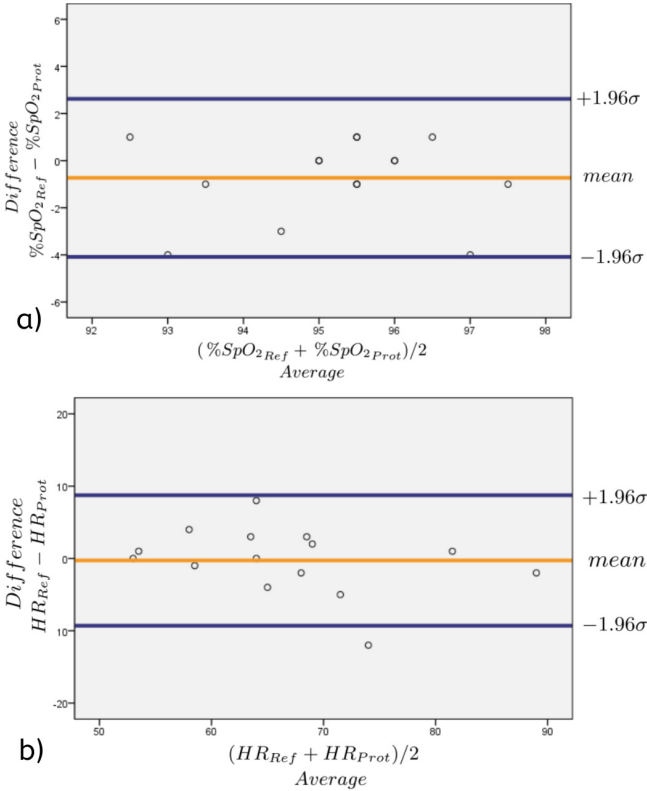


Fig. 5. Bland-Altman plots for a) SpO_2 measurements and b) HR measurements.

between the SpO_2 and HR measurements of both oximeters had a p value of $p > 0.05$, which indicates that they are not statistically significant. As for the Bland-Altman analysis, the dispersion graphs were made by plotting the differences between the reference measurements (*Ref*) and those of the prototype (*Prot*) against their corresponding average values. The confidence intervals which group 95% of the data were plotted at ± 1.96 standard deviation (σ) from the average value of the differences as shown in Fig. 5 [8].

It is clear that the Bland-Altman analysis show different results from those reported in Table 1. This difference can be attributed to several factors, but

mainly it is due to the different methodology follow in the pilot test. Whereas in validation tests measurements from the prototype and the reference oximeter were recorded just once, those of the pilot test were recorded three times separated by 2 min, and since the values of SpO_2 and HR are not static, the results displayed by the prototype can be different because the response time of each oximeter is not the same. In any case, this does not imply a greater error.

4 Conclusions

An optimized performance pulse oximeter based on the MAX30102 was obtained. The developed prototype meets the technical and functional requirements established by the Pan American Health Organization for clinical pulse oximeters. Results show that the proposed algorithms calculate SpO_2 and HR with one-unit resolution and accuracies of 1.39% and 2.04 bpm, respectively.

Two algorithms to calculate HR were proposed. The FFT showed a better performance than the intensity based algorithm for PPG signals with low SNR values and fake peaks induced by movement. However, to guarantee its correct operation, a microcontroller with greater SRAM memory capacity must be used. Finally, the Bland-Altman analysis of the pilot test results indicate that the measurements of the prototype are comparable to those of a high-end commercial oximeter. However, it is advisable to carry out a validation with a larger number of people.

Conflict of Interest. The authors declare that they have no conflict of interest.

Acknowledgments. The authors acknowledge financial support from UNAM-PAPIIT grant iv100320 and SECTEI grant SECTEI/080/2020. Ricardo Cebada-Fuentes and José Valladares-Pérez thank CONACYT for the Ph.D. studies grant (CVU:1005230) and (CVU:929080).

References

1. Chan, E.D., Chan, M.M., Chan, M.M.: Pulse oximetry: understanding its basic principles facilitates appreciation of its limitations. *Respir. Med. (Elsevier)* **107**, 789–799 (2013)
2. Allen, J.: Photoplethysmography and its application in clinical physiological measurement. *Physiol. Meas.* **28**, R1 (2007)
3. Badgujar, K.C., Badgujar, A.B., Dhangar, D.V., Badgujar, V.C.: Importance and use of pulse oximeter in COVID-19 pandemic: general factors affecting the sensitivity of pulse oximeter. *Indian Chem. Eng.* **62**, 374–384 (2020)
4. Webster, J.G.: *Design of Pulse Oximeters*. CRC Press (1997)
5. Shruthi, P., Resmi, R.: Heart rate monitoring using pulse oximetry and development of fitness application. In: 2nd International Conference on Intelligent Computing, Instrumentation and Control Technologies (ICICT), vol. 1, pp. 1568–1570. IEEE (2019)
6. Andika, I.P.A., Rahmawati, T., Mak'ruf, M.R.: Pulse oximeter portable. *J. Electron. Electromed. Eng. Med. Inf.* **1**, 28–32 (2019)

7. Integrated Maxim: Recommended Configurations and Operating Profiles for MAX30101/MAX30102 EV Kits. www.maximintegrated.com/en/design/technical-documents/userguides-and-manuals/6/6409.html (2018)
8. Kaur, P., Stoltzfus, J.C.: Bland-Altman plot: a brief overview. *Int. J. Acad. Med.* **3**, 110 (2017)
9. Pan American Health Organization: Technical and Regulatory Aspects of the Use of Pulse Oximeters in Monitoring COVID-19 Patients
10. Integrated Maxim. MAX30102 Datasheet. www.maximintegrated.com/en/products/interface/sensor-interface/MAX30102.html
11. Fine, J., Branan, K.L., Rodriguez, A.J., Boonya-Ananta, T., Ramella-Roman, J.C., McShane, M.J.: Sources of inaccuracy in photoplethysmography for continuous cardiovascular monitoring. *Biosensors* **11**, 126 (2021)
12. Ley General de Salud and CAPITULO ÚNICO. Ley General de Salud
13. Skrvan, A., Hudec, R., Matuska, S.: Design of a cheap pulse Oximeter for home care systems. *ELEKTRO (ELEKTRO)*, pp. 1–6. IEEE (2022)
14. Prada, A., Javier, E., Maldonado, S., Daniel, R.: A novel and low-complexity peak detection algorithm for heart rate estimation from low-amplitude photoplethysmographic (PPG) signals. *J. Med. Eng. Technol.* **42**, 569–577 (2018)
15. Rao, K.R., Kim, D.N., Hwang, J.J.: *Fast Fourier Transform: Algorithms and Applications*. Springer (2010)
16. Sani, N.H.M., Mansor, W., Lee, K.Y., Zainudin, N.A., Mahrim, S.A.: Determination of heart rate from photoplethysmogram using Fast Fourier transform. In: *International Conference on BioSignal Analysis, Processing and Systems (ICBAPS)*, pp. 168–170. IEEE (2015)
17. Zonst, A.E.: *Understanding the Fast Fourier Transform: Applications*. Citrus Press (1995)